Membrane dynamics of Procyclin and effect of CC2D on plasma membrane of *Trypanosoma brucei* by z-scan FCS and FCS Diffusion Laws

MS Thesis

Academic Year 2016-17

By

Aditya Katti (20121092)

BS-MS Dual degree program

Thesis supervisor: Prof. Cynthia He, NUS
Co-supervisor: Prof. Thorsten Wohland, NUS
Thesis advisor: Dr. Shivprasad Patil, IISER

Certificate

This is to certify that this dissertation entitled “Membrane dynamics of Procyclin and effect of CC2D on plasma membrane of *Trypanosoma brucei* by z-scan FCS and FCS Diffusion Laws” towards the partial fulfillment of the BS-MS dual degree program at the Indian Institute of Science Education and Research, Pune represents original research carried out by Aditya Katti at National University of Singapore, Singapore under the supervision of Dr. Cynthia He, Associate Professor, Department of Biological Sciences, National University of Singapore and Dr. Thorsten Wohland, Professor, Centre for Bio-Imaging Sciences, Depatrment of Biological Sciences, National University of Singapore during the academic year 2016-2017.

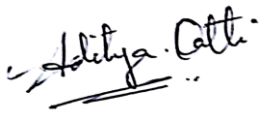

19 March, 2017

Aditya Katti
Registration number: 20121092
BS-MS Dual Degree Student
IISER Pune
(2016-2017)

Dr. Cynthia He
Associate Professor
Cellular and Molecular Parasitology Lab
Department of Biological Sciences
National University of Singapore

Declaration

I hereby declare that the matter embodied in the report entitled “Membrane dynamics of Procyclin and effect of CC2D on plasma membrane of *Trypanosoma brucei* by z-scan FCS and FCS Diffusion Laws” are the results of the investigations carried out by me at the Department of Biological sciences, National University of Singapore, Singapore under the supervision of Dr. Cynthia He and Dr. Thorsten Wohland, Professor, Centre for BioImaging Sciences, Depatrment of Biological Sciences, National University of Singapore and the same has not been submitted elsewhere for any other degree.

19 March, 2017

Aditya Katti
Registration number: 20121092
BS-MS Dual Degree Student
IISER Pune
(2016-2017)

Dr. Cynthia He
Associate Professor
Cellular and Molecular Parasitology Lab
Department of Biological Sciences
National University of Singapore

Table of Contents

Abstract

Membrane dynamics of Procyclin, a GPI-anchored protein in *Trypanosoma brucei* has been studied for the first time by z-scan FCS and FCS Diffusion Laws. The τ_0 for procyclin is ~6.8 ms which indicates a cholesterol-dependent nanodomain confinement which on depletion by MβCD gives a τ_0 of ~1.6 ms and is ~2.1 ms at 24 hours post CC2D-RNAi and reduces further to ~0.6 ms at 48 hours post CC2D-RNA interference. Dynamics after knockdown of CC2D by RNA interference resembles cholesterol depletion by MβCD on plasma membrane of *Trypanosoma brucei*.

List of Figures

List of Tables

Acknowledgments

I would first like to thank IISER, Pune for this amazing opportunity to do my MS thesis in NUS, Singapore. I would like to thank Prof. Cynthia He and Prof. Thorsten Wohland for giving me this opportunity to learn and work in their labs and gain insight in the fields of Cell and Molecular Biology and Biophysics. Their constant support and motivation has enabled me to venture and explore parts of biology and the importance of physical quantitation methods in the present research community in biology. I would like to Xue Wen Ng, graduate student in Prof. Wohland's lab for her invaluable advice and guidance during my project. Her hardworking nature and inquisitiveness has inspired me to do the same and I have developed my work ethic because of her. I would like to thank Dr. Shen Qian, former graduate student in Dr. He's lab for her indispensible effort in helping me learn the concepts involved in the cell and molecular biology, especially *Trypanosoma brucei*. Her constant support in providing me with samples has helped me sustain my project till the end. I would also like to thank all the other lab members in both the labs for their support. I would like to thank Mei Lin Kwong and Kai Jie Koh for their company in the lab during experiments and discussions. I would like to thank Abhishek Anand, IISER student and my roommate and Vishal Bhagat, graduate student in Prof. He's lab who gave me useful insight in biology which gave me a better sense in my work involved. Lastly, I would like to thank all my friends and family for their unwavering love and support during this period. This opportunity has helped me mold myself into a more able research student and I believe I will continue venturing in the field of research.

Introduction

Trypanosoma brucei is a single-celled, eukaryotic parasite known to cause African sleeping sickness in humans and Nagano in cattle. The study of these and related pathogens is important in the field of medical research. Two proliferative life cycle forms are commonly used for lab studies, the procyclic form (PCF) and the bloodstream form (BSF). The former is found in the tsetse fly midgut and the latter in the blood of humans and cattle through transmission by infected tsetse fly. It has a prominent flagellum and single-copy of the organelles. It is an ideal model organism for understanding concepts in cell biology such as organelle biology, cell morphogenesis and flagellum biogenesis. Reasons could include that it is genetically tractable, that is it has a fully sequenced genome and it is easy is to manipulate it by point mutations, endogenous replacement of DNA, knockdown of certain proteins to name a few. Also, since these organisms are easy to culture, it is convenient to use them.

The flagellum attachment zone (FAZ) is also known as the ‘cellular ruler’ due to its position and function as it coordinates organization, biogenesis and dynamics of cytoskeletal and membrane-like components of the cell. *T. brucei* maintains its structural integrity, motility and division by a microtubule-based cytoskeleton contrary to mammalian cells which have an actin cytoskeleton for the same. Actin is only involved in a few processes mainly in endocytosis (Garcia-Salcedo et al., 2004). Apart from associating to microtubule cytoskeleton, it is associated to the flagellar membrane and the plasma membrane by joining these two membranes. It is adjacent to the FAZ-ER, which coordinates with the single Golgi apparatus present in the cell. The flagellar pocket (FP) is an invagination in the plasma membrane where all endocytosis and exocytosis events take place. This is part of the endosomal system which involves the Golgi apparatus too (inset-top left). Thus we can see that there is an interconnection between the membrane and cytoskeleton (Fig. 1).

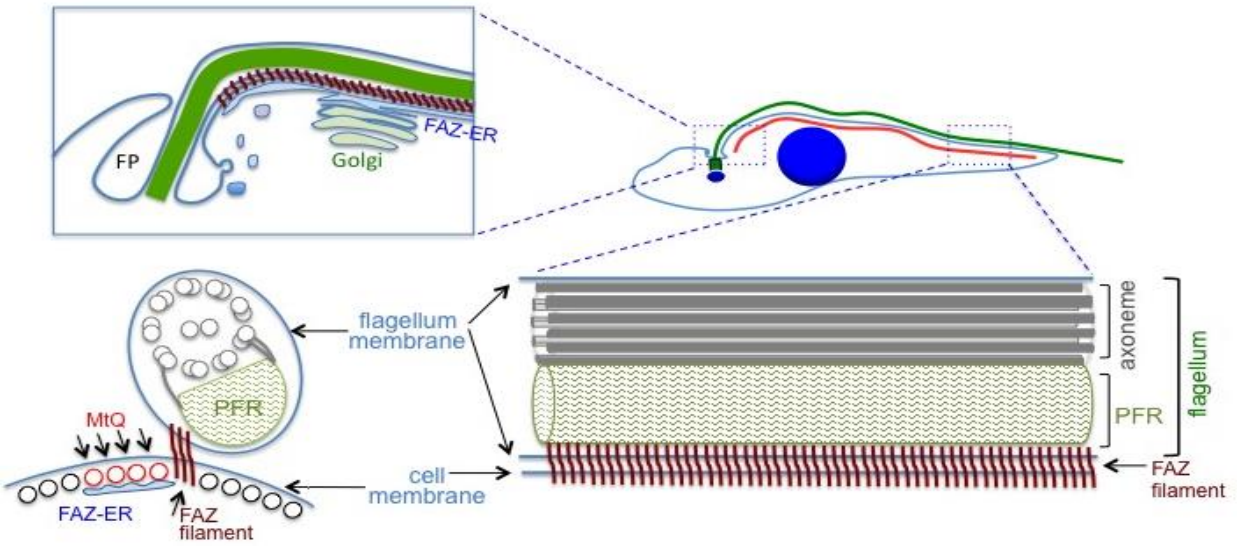

Fig. 1. The organization of the FAZ complex relative to other cytoskeletal and membraneous structures in the cells. *T. brucei* cell has a distinct auger shape, with polarized cellular organization (top right). A single flagellum (green) is laterally attached to the cell body, via a FAZ complex (red). At the base of the flagellum and FAZ complex, the plasma membrane folds into a flask shaped flagellar pocket (FP; top left), where endocytosis and exocytosis take place. Many vesicles and endosomal structures are found between the FP and the single Golgi stack adjacent to the FAZ-ER (inset on top left). Both cross (bottom left) and side view (bottom right) of the flagellum-FAZ nexus are shown side by side. Flagellum, green line; FAZ, red line; basal body, green box; kinetoplast (mitochondrial DNA), small blue dot; nucleus, large blue circle. The FAZ contains electron-dense filament, and the MtQ (the sub-pellicular microtubule quartet) in close association with FAZ-ER (light blue). (Adapted from Prof. Cynthia He)

Previous studies done related to FAZ have been in relation to the cytoskeletal organization and its effect on morphology of the cell (Zhou et al., 2011; Sunter et al., 2015). FAZ function in membrane organization has not been probed in detail until recently. *T. brucei* orthologue of VAMP-associated proteins TbVAP was found to be at the FAZ filament and FAZ-ER. Depletion of TbVAP disturbed the architecture of FAZ-ER, but the cell cycle and the cell viability remained unaffected (Lacomble et al., 2012). Discovery of CC2D, a coiled-coil and C2 domain containing protein that is essential for cell growth and is stably associated with the FAZ is a good system to dissect the function of FAZ-membrane association. CC2D is present on the FAZ filament, FAZ-juxtaposed ER membrane and the basal bodies. The coiled coils are generally known to be involved in protein oligomerization. The C2 domain is implicated in membrane

interactions. Depletion of CC2D inhibits the assembly of a new FAZ filament, forming a small FAZ region with a relatively fixed size at the base of a detached flagellum. Inhibition of new FAZ formation perturbs subpellicular microtubule organization and generates short daughter cells (Zhou et al., 2011).

Most of the C2 domain-containing proteins are involved in membrane trafficking or signal transduction. They are the second most abundant lipid binding domain after the PH domain. Generally, C2 domain proteins are soluble proteins while some proteins involved in membrane trafficking with multiple C2 domains are transmembrane proteins. Some C2 domains do not have affinity to Ca^{2+}, i.e. they do not have Ca^{2+}-dependent membrane binding. Most of these Ca^{2+}-independent C2 domains are involved in protein-protein interactions or are non-functional, while some are involved in membrane binding (Cho and Stahelin, 2006).

Liposome pull-down experiments done for the entire C2 domain showed the CC2D-C2 domain binds to lipids independent of presence of Ca^{2+} ions as it precipitated with the liposomes in the presence and absence of Ca^{2+} ions (unpublished) (Fig.2). Lipid blot assays further confirmed binding with different lipids, namely phosphatidic acid, phosphatidylserine and cardiolipin. All these are negatively charged, acidic lipids (unpublished) (Fig. 2).

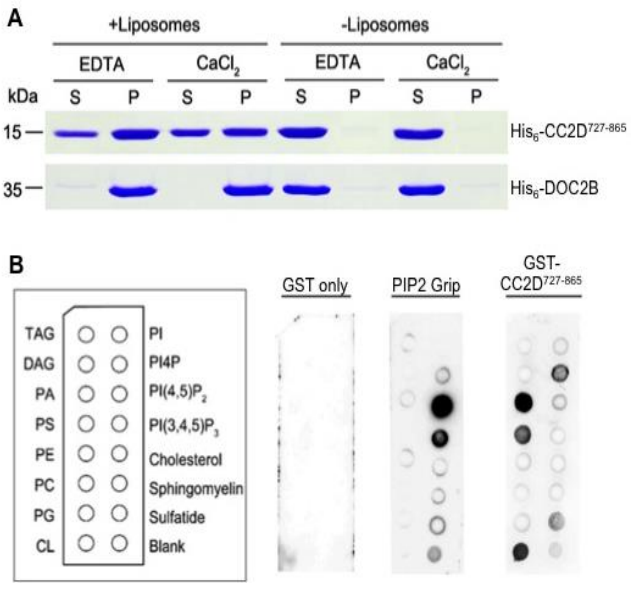

Fig. 2. CC2D-C2 domain interacts with lipids in a Ca2+-independent manner. A. 2 μg/ml each of His_6-$CC2D^{727-865}$ and His_6-DOC2B (positive control) was mixed with liposomes in the presence of 100μM $CaCl_2$ or 100μM EDTA. The pellet (containing liposomes) and supernatant fractions were analyzed by SDS-PAGE. **B**. Lipid blots were incubated with GST-$CC2D^{727-865}$, with GST only and GST-PIP2 Grip as controls. TAG, triglycerides; DAG, diacylglycerol; PA, phophatidic acid; PS, phosphatidylserine; PE, phosphoethanolamine; PC, phosphotidylcholine; PG, phosphatidylglycerol; CL, cardiolipin; PI, phosphatidylinositol; PI4P, PtdIns(4)P; $PI(4,5)P_2$, $PtdIns(4,5)P_2$; $PI(3,4,5)P_3$, $PtdIns(3,4,5)P_3$. (With permission from Prof. Cynthia He)

CC2D-C2 domain lipid-affinity being established, further studies were done to see how it affected lipid organization. Different lipids were examined with suitable markers; for example, YFP-PH_{Tapp1} (M52b) for PI(3,4)P2 and filipin for cholesterol to understand how knocking-down CC2D affected their organization. Filipin fluorescence intensity significantly decreased on the plasma membrane and flagellar membrane. Moreover, calflagin, a lipidated protein which targets to the enriched sterol in the flagellar membrane (Tyler et al., 2009) was disrupted (unpublished).

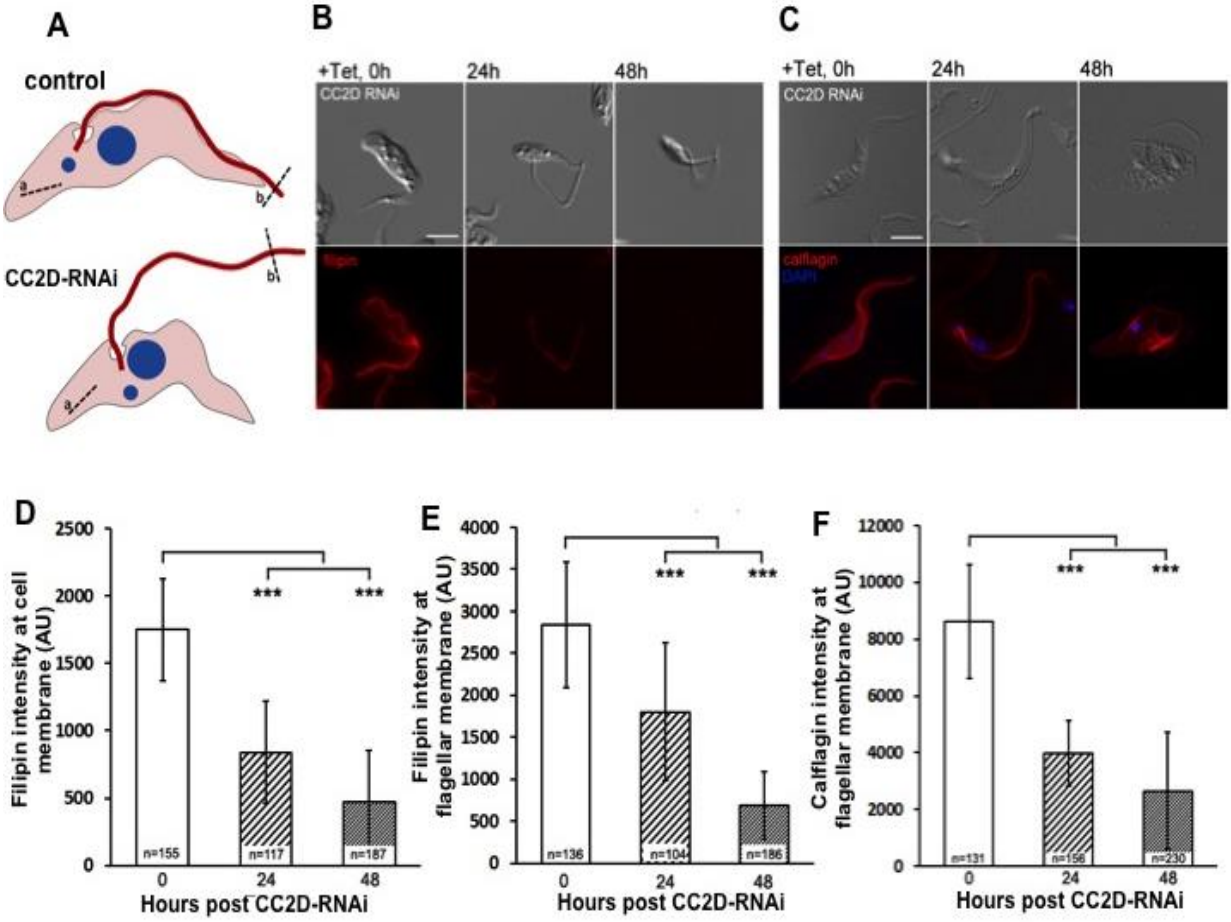

Fig. 3. CC2D is required for membrane lipid organization and flagellar membrane protein localization. A-C. Control and CC2D-RNAi cells were stained with filipin to monitor membrane sterol distribution and abundance (**B**), or stably transfected with mCherry-calflagin, T24, a flagellar membrane protein that relies on flagellar membrane lipid organization from proper targeting (**C**). Fluorescence intensity on cell membrane (line *a* in **A**) and flagellar membrane (line *b* in **A**) was quantitated for filipin or mCherry-calflagin, T24 in control and CC2D-RNAi cells. **D-F**. Quantitation results were shown as mean±SD. Cell numbers were indicated at the bottom of each column. Each measurement was repeated at least 3 times. (With permission from Prof. Cynthia He)

Here, an attempt has been made to understand the effects of CC2D on plasma membrane dynamics and the lipid organization on the plasma membrane of T.brucei by z-scan fluorescence correlation spectroscopy (zFCS) (Humpolícková et al., 2006) and FCS diffusion laws (Wawrezinieck et al., 2005).

Theory

Fluorescence Correlation Spectroscopy (FCS)

Fluorescence Correlation Spectroscopy (FCS) is a tool which can be used to understand membrane diffusion properties by analyzing fluorescence fluctuations and fitting to an equation known as the autocorrelation function (Haustein and Schwille, 2007)

$$G(\tau) = \frac{\langle F(t)F(t+\tau)\rangle}{\langle F(t)\rangle^2} = \frac{\langle F(0)F(\tau)\rangle}{\langle F(t)\rangle^2} = \frac{\langle \delta F(t)\delta F(t+\tau)\rangle}{\langle F(t)\rangle^2} + 1 \qquad \text{(Equation 1)}$$

Where, $\langle F(t)\rangle = \frac{1}{T}\int_0^T F(t)dt$

Where $\mathrm{F(t)}$ is the fluorescence signal at time t, τ is the lag-time and $\delta F(t) = F(t) - \langle F(t)\rangle$. This is the experimental equation for the autocorrelation function.

The fluorescence F produced by a single chemical species that diffuse is given by the diffusion equation

$$\frac{\partial}{\partial t}\delta C(r,t) = D\nabla^2\delta C(r,t) \qquad \text{(Equation 2)}$$

Where, $\delta C(r,t) = C(r,t) - < C(r,t) >$ is the concentration fluctuation function as a function of time t and diffusion coefficient D. These concentration fluctuations are related to fluorescent fluctuations by

$$\delta F(t) = I_0(r_0 = 0)\int S(r_0)\Omega(r_0)\delta(q\sigma C(r_0,t)\, dr_0 \qquad \text{(Equation 3)}$$

Where $\mathrm{I_0}$ is the illumination profile, S is the normalized illumination profile, Ω is the collection efficiency profile, $\mathrm{r_0}$ is the position in object space, q is the quantum yield, σ is

the extinction coefficient and C is the concentration. The normalized observation volume profile is defined as $O(r_0) = S(r_0)\Omega(r_0)$. The illumination profile is a 3D Gaussian given approximately by (Aragón and Pecora, 1975)

$$\left[O(r,z) \sim e^{-\left(\frac{r}{r_0}\right)^2} e^{-\left(\frac{z}{z_0}\right)^2}\right]$$

The $1/e^2$ decay in the radial direction is given by r_0 and in the axial direction is given by z_0. For 3D free diffusion of a population of monodisperse fluorophores, $G(t)$can be obtained by solving equation 1 (Elson and Magde, 1974)

$$G(t) = \frac{1}{N}\left(\frac{1}{1+\frac{\tau}{\tau_D}}\right)\left(\frac{1}{1+\frac{\tau}{\tau_D}\left(\frac{r_0}{z_0}\right)^2}\right)^{\frac{1}{2}} \qquad \text{(Equation 4)}$$

Where, N is the number of particles in the confocal volume of radius r_0 and height z_0, determined by the illumination profile of the diffraction limited spot.

The average amount of time spent by the fluorophore in the confocal volume is given by the diffusion time, τ_D which is related to the diffusion coefficient, D by the following equation (Haustein and Schwille, 2007)

$$D = \frac{r_0^2}{4\tau_D} \qquad \text{(Equation 5)}$$

Fluorophores also exhibit a blinking state where the fluorophore enters the first excited triplet state on excitation. Since this can happen when the fluorophore is in the confocal volume, it adds a component to the autocorrelation curve and to the analysis. This additional decay component is a factor which characterizes the triplet state kinetics and is given by

$$G(\tau) = 1 + \frac{T}{1-T}e^{-\frac{\tau}{\tau_{trip}}} \qquad \text{(Equation 6)}$$

τ_{trip} is the relaxation time of the triplet state, T is the fraction of the fluorophore in the triplet state

Hence, for a dye freely diffusing in the confocal volume the autocorrelation function $G(\tau)$ is given by

$$G(t) = \frac{1}{N}\left(\frac{1}{1+\frac{\tau}{\tau_D}}\right)\left(\frac{1}{1+\frac{\tau}{\tau_D}\left(\frac{r_0}{z_0}\right)^2}\right)^{\frac{1}{2}}\left(1 + \frac{T}{1-T}e^{-\frac{\tau}{\tau_{trip}}}\right) \qquad \text{(Equation 7)}$$

This function has been used for calibration of the observation/confocal volume for different lasers used. Determining r_0 from a dye of known diffusion coefficient D, and τ_D obtained from the FCS of the dyes.

For diffusion in 2D (membranes, etc), $r_0 \to \infty$ which implies that $\left(\frac{r_0}{z_0}\right) \to 0$ and for a fluorophore exhibiting a triplet state, the autocorrelation function which is given by

$$G(\tau) = \frac{1}{N}\left(1 + \frac{\tau}{\tau_D}\right)^{-1}\left(1 + \left(\frac{T}{1-T}\right)e^{-\frac{\tau}{\tau_{trip}}}\right) + G_\infty \qquad \text{(Equation 8)}$$

G_∞ is the autocorrelation at infinite time.

FCS in the early lag times (~10^{-5}-10^{-4} ms) show detector artifacts namely afterpulsing which give correlations in those lag times. Detector signal pulse due to a real signal may be followed by a pulse at a later time, called an afterpulse (Zhao et al, 2003).

Timescales ranging from a few microseconds onwards give us essential data on triplet state dynamics, free diffusion of dyes and membrane diffusion to name a few phenomena.

FCS is useful for measuring molecular dynamics in biology and especially membrane dynamics. It has its own disadvantages, one of them being that we need to have prior knowledge of the system we are looking at to accurately quantify its interactions.

Fluorescence photobleaching has been an issue for FCS measurements all the time. Multiple models can give similar fits. Also, over-fitting of data would give us incorrect interpretations. Additionally, conventional FCS measurements are limited by the optical diffraction limit and length scales of below 200 nm cannot be probed. (Ng et al., 2015). However, structures in the membrane like lipid rafts/ nanodomains have much smaller sizes (Pike, 2006).

FCS Diffusion Laws

FCS diffusion laws can give us a better understanding of the model as we are observing the diffusion at different length scales. It depends on varying the observation volume and the diffusion behavior of the molecules being probed by the structures in the membrane. Previous experiments of the same kind have been done in fluorescence recovery after photobleaching (FRAP) which have shown existence of micrometer sized domains in fibroblast plasma membranes (Yechiel and Edidin, 1987). In a freely diffusing system, the diffusion of the probes the observed area is directly proportional to the area. At zero spot-width, the diffusion time of the probe will be seen as zero in the diffusion law plot. This relation may not hold for heterogeneous media. Simulations were done varying domain densities, sizes, probability of crossing barriers of the domains and confinement strength. Confinement strength is defined as the ratio of diffusion time in confinement to free diffusion time in the domain. Diffusion time in confinement is the time required for the particle to escape the domain. The diffusion law plots all show a positive deviation from zero at near-zero observation areas. This was also backed by experiments. Similarly for confinement in a meshwork, simulations were done varying mesh sizes, probability of crossing the barrier, different confinement strengths. The mesh is assumed to be square-shaped with domains between them. The diffusion law plots all show a negative deviation from zero at near-zero observation areas.

Since we cannot access the zero spot-width physically due to the diffraction limit, extrapolating the linear plot need not give a zero intercept and it may either be positive or negative, indicating different diffusion behaviors. If it is a positive intercept, it may be

indicative of domain confinement of the probe in question. If it gives a negative intercept, it may be confinement within the actin cytoskeleton (Wawreznieck et al., 2005) (Fig.4). FCS diffusion law plots have been generated by plotting τ_D and r_0^2, except for determining the zero spot-width from the POPC bilayer where τ_D and Δz^2 has been used as shown in the Results and Discussion.

The τ_0 value is only indicative of the kind of confinement or the kind of dynamics the molecule has and has no physical significance on its own. Hence, control experiments are absolutely necessary to understand the confinement values. These are purely based on experimental and simulation based results.

Z-scan FCS (zFCS)

FCS diffusion law measurements can be performed with different modalities. Incorporating nanometric apertures (Wenger et al., 2007), inserting diaphragms at the back aperture of the objective or changing the spot-width manually (Wawrezinieck et al., 2005; Lenne et al., 2006) can give an accurate estimate of the observation area, which is necessary for the diffusion law plot. But in commercially available confocal-FCS systems, incorporating such changes may not be feasible. The z-scan approach introduced by Humpolícková et al. (2006) and subsequently followed by Ganguly et al. (2010) is a convenient method for the measurements made under the constraints of the commercial system. The principle of zFCS is scanning the divergent light beam along the z-axis to obtain variable observation areas and then performing the FCS measurement.

The diffusion time measured by FCS has a parabolic dependence with different planes in the z-direction for a Gaussian intensity profile of the illumination. The dependence is given by (Humpolícková et al., 2006)

$$\tau_D = \frac{r_0^2}{4D}\left(1 + \frac{\lambda_0^2 \Delta z^2}{\pi^2 n^2 r_0^4}\right) \qquad \text{(Equation 9)}$$

λ_0 is the excitation wavelength, n is the refractive index and $\Delta z = z - z'$ is the distance between the sample position (z) and the position of focus (z') where the beam radius is r_0. The vertex of the parabola is the diffusion time of the system at $z = z'$. The diffusion times are plotted against the z-position and fit with the equation

$$\tau = \tau_0 + \frac{r_0^2}{4D}\left(1 + \frac{\lambda_0^2 \Delta z^2}{\pi^2 n^2 r_0^4}\right) \qquad \text{(Equation 10)}$$

The lowest diffusion time will correspond to the measurements done where the membrane is in focus.

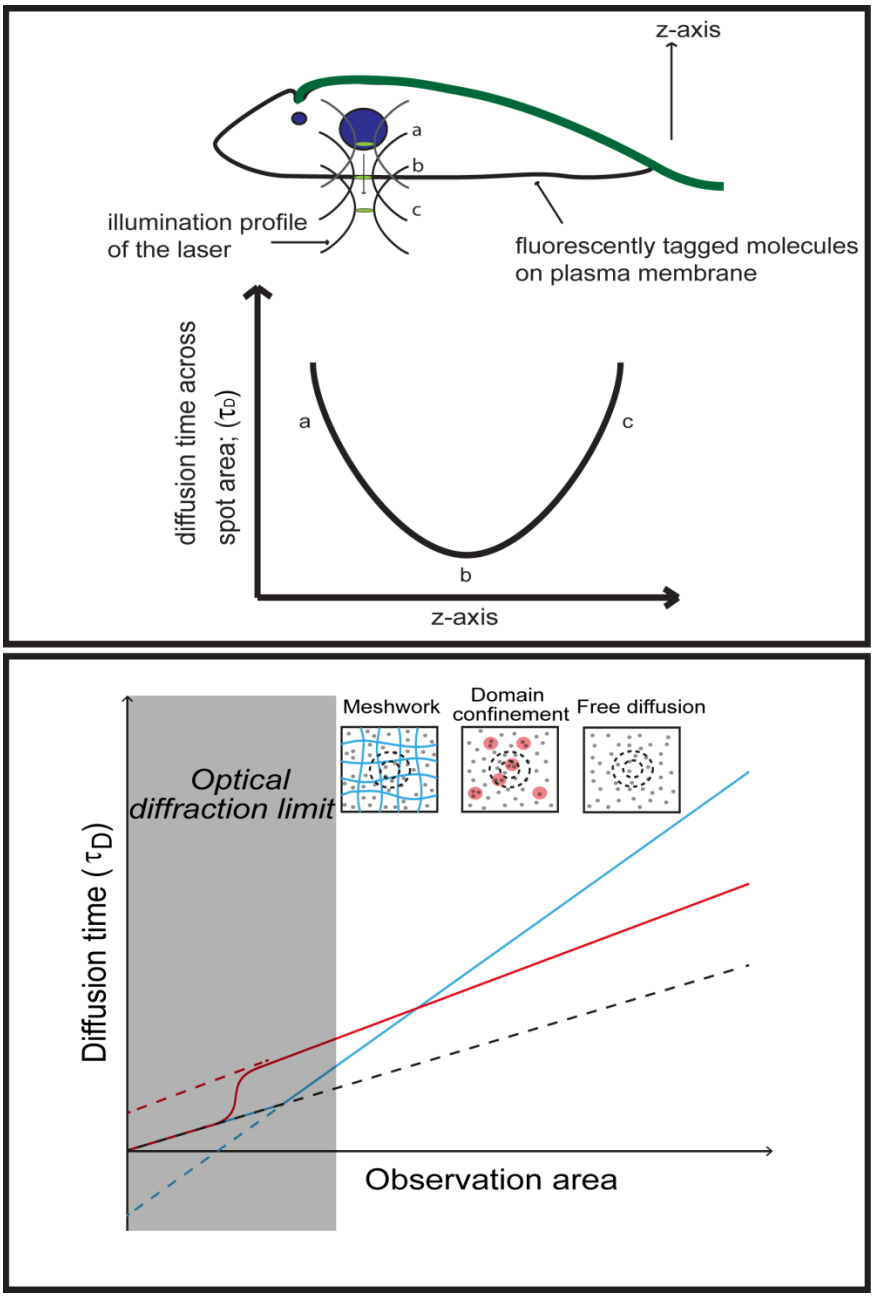

Fig. 4. Depiction of zFCS and FCS Diffusion Law. (A) zFCS is a method where the diffraction-limited spot is moved along the z-axis and FCS measurements are done to determine τ_D, the diffusion time of the fluorophore across the observation volume. The trypanosome is depicted showing the kinetoplast (blue dot), nucleus (blue circle), a flagellum (green line) and a fluorescently-tagged membrane. The observation volume increases as the focus is shifted across the z-axis which increases the area in a parabolic scale with the z-shift. The τ_D scales in a similar parabolic scale as τ_D is directly proportional to the square of the radius of the spot. The focused spot is point 'b' which gives the least diffusion time and points 'a' and 'c' are the points with the larger observation volumes and hence larger diffusion times. **(B)** Given are typical diffusion law plots which have been found through simulations done by Wawrezinieck et al. (2005) for different modes of diffusion of the fluorophore. The intercepts are extrapolated by the diffusion law plots as we cannot access observation areas below the diffraction limit. Black dotted circles depict the different observation volumes and the grey dots are the fluorophores. The free diffusion regime is characterized by an intercept which goes to zero as the observation area goes to zero (black dotted line). The domain-confined (red-circles) regime is characterized by a positive intercept on extrapolation. The meshwork-confined (blue grids) regime is characterized by a negative intercept on extrapolation. (FCS Diffusion Law figure adapted from Ng Xue Wen, NUS Graduate student, with permission)

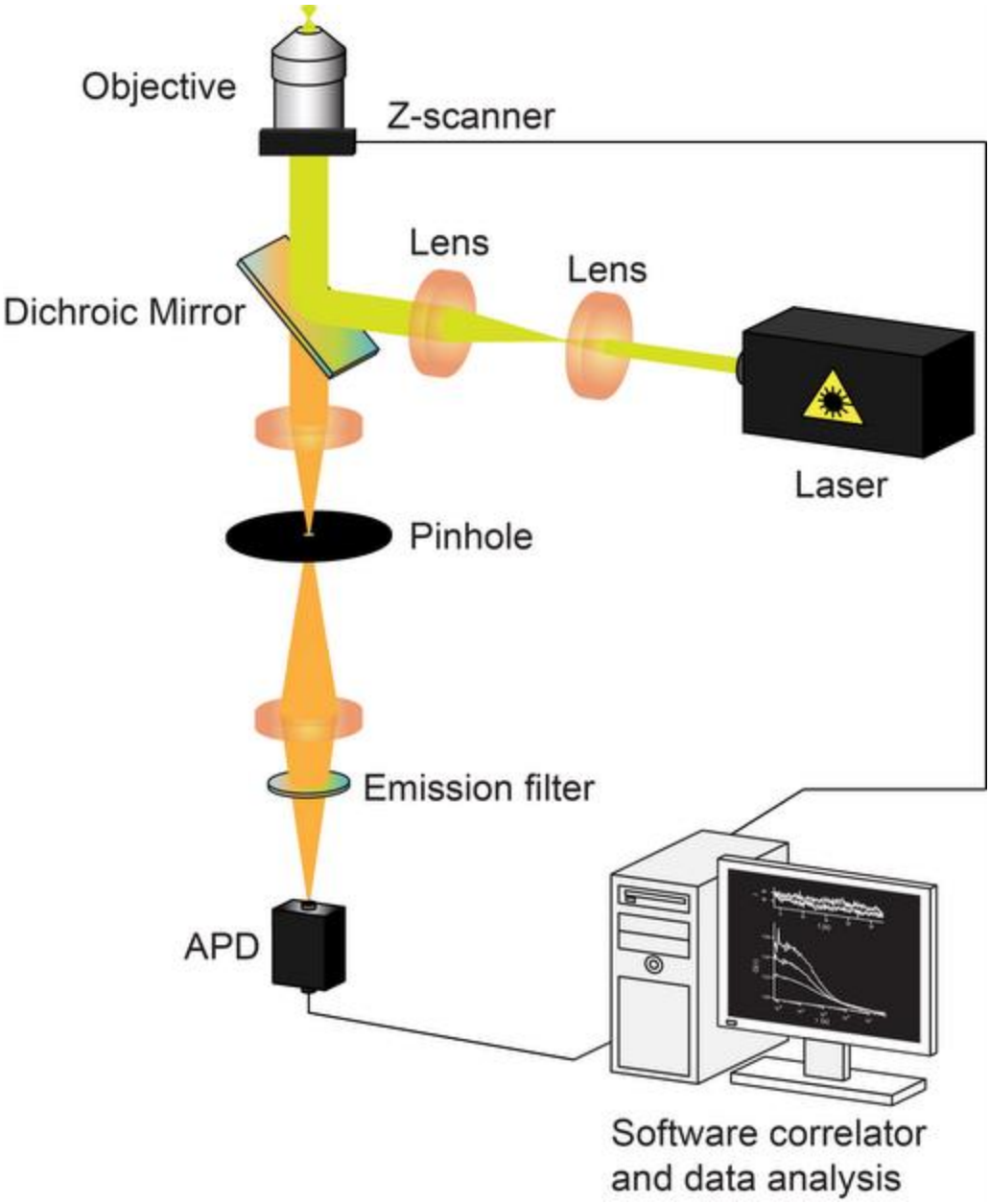

Fig. 5. Setup of Confocal Microscope for Confocal FCS and zFCS. The laser spot is collimated and is reflected on the dichroic mirror which is then focused by a high numerical aperture, high magnification objective which forms the observation volume. Fluorophores diffusing into the observation volume emit fluorescence which is collected by the same objective and the emitted wavelengths are selected for by the dichroic mirror to be transmitted. This light is focused into a pinhole and the beam is further cleaned up by the emission filter to further remove the unwanted wavelengths. It is then focused on to an avalanche photodiode (APD, also called SPAD) for collecting the light and then processed and analyzed on the computer with a software correlator. The objective has a z-scanner unit which is used to move it in steps of nanometers, necessary for zFCS. The pinhole helps in selecting for the different planes on the z-axis which is important for zFCS application. (Adapted from Dr. Foo Yong Hwee's PHD thesis)

Materials and Methods

z-Scan FCS (zFCS) Measurements and Analysis; Fluoresence Imaging of Trypanosomes

All experiments were performed on a commercially available Olympus FV1200 laser scanning confocal microscope (IX83; Olympus, Singapore). The 543 nm laser beam (Olympus, Singapore) was focused on the sample by a water immersion objective (UPLSAPO, 60×, NA 1.2; Olympus, Singapore) after being reflected by a dichroic mirror (DM405/488/543/635 band pass; Olympus, Singapore). The fluorescence from the sample passes through the 120 µm pinhole, filtered by a 600/50-25 emission filter (Semrock, Rochester, NY, USA). The calibration for FCS was done using Atto565 (AttoTec GmbH, Germany) dye (D = 426 $\mu m^2 s^{-1}$) (Müller et al., 2008). The 515 nm Argon-ion multi-line laser beam (Melles Griot, Singapore) passes through the same objective after being reflected by a dichroic mirror (DM455/515 band pass; Olympus, Singapore). The fluorescence from the sample passes through the 120 µm pinhole, filtered by a 534/30-25 emission filter (Semrock, Rochester, NY, USA). The calibration for FCS was done using Rhodamine 6G (R6G) (Sigma Aldrich, Singapore) dye (D = 414 $\mu m^2 s^{-1}$) (Müller et al., 2008). The fluorescence intensities were recorded by a single molecule avalanche photodiode (SPAD) (SPCM-AQR-14, PerkinElmer Optoelectronics, Quebec, Canada). Acquisition time for the correlations ranged from 10 s to 20 s. The z-scan was performed in steps of 100 nm, 0.7 µm into and 0.7 µm away from the sample for the POPC-Rhodamine-PE bilayers and in steps of 200 nm, 1 µm into and 1 µm away from the sample for the YFP-Procyclin/DiI-stained trypanosomes.

Fluorescence images of trypanosomes were taken at a scan speed of 20 µs/s for a region of interest of 52.6 x 52.6 μm^2 with 512x512 pixels at a final magnification of 240x. The fluorescence from the sample was recorded by a photomultiplier tube after the light is filtered by an emission bandpass filter (BA 560-605 for DiI-C_{18} and BA535-565 for

R6G; Olympus, Singapore). Images were untreated and minor modifications were made in ImageJ (NIH, USA).

Fitting and Statistical analysis

The signals were processed to obtain and fit the autocorrelation function (ACF) by the Symphotime 400 software (PicoQuant GmbH, Berlin, Germany) using equation 6 for the trypanosomes and the POPC bilayer to determine the diffusion times (τ_D) of DiI and YFP-Procyclin in the trypanosomes and Rhodamine-PE on the POPC bilayer. The ACFs were fitted for lag times of 0.01 ms to ~100-1000 ms and was represented in Origin 9.0 (OriginLab Corp., Northampton, MA).

For the POPC bilayers, the fitting equation used was

$$\tau = \tau_0 + b\Delta z^2 \qquad \text{(Equation 11)}$$

All Δz^2 have been subsequently converted to r^2 values to give a more comprehensive idea of the spot area in the diffusion law plots for the trypanosomes and is given by

$$r^2 = r_0^2\left(1 + \frac{\lambda_0^2 \Delta z^2}{\pi^2 n^2 r_0^4}\right) \qquad \text{(Equation 12)}$$

Equation 9 gives the relation used for fitting the diffusion law, i.e. between τ_D and r_0^2

$$\tau = \tau_0 + ar_0^2 \qquad \text{(Equation 13)}$$

The z-scan plots and diffusion laws were fit and plotted in Origin 9.0 (OriginLab Corp., Northampton, MA). Statistics were done in Microsoft Excel and Origin 9.0.

Preparation of Supported Lipid Bilayers (SLBs)

1-Palmitoyl-2-oleoylphosphatidylcholine (POPC) is the lipid and 1,2-dimyristoyl-sn-glycero-3-phosphoethanolamine-N-(lissamine rhodamine B sulfonyl) (ammonium salt) (Rho-PE, λ_{ex}= 557 nm and λ_{em} = 571 nm) was the fluorophore used for the preparation of the SLBs (Avanti Polar Lipids, Alabaster, AL). They were prepared by the vesicle fusion method (Brian and McConnell, 1984). Calculated amounts of lipid and dye solutions were mixed together in a round-bottom flask and the solvent was evaporated using a rotary evaporator (Rotavap R-210, Buchi, Switzerland) for 2-3 hours. The thin lipid film obtained is then dissolved in 2 mL buffer containing 10 mM HEPES and 150 nM NaCl at pH 7.4. Small unilamellar vesicles (SUVs) were prepared by sonicating from the turbid suspension until it cleared using a bath sonicator (FB15051 Model, Fisher Scientific, Singapore). 200 µL of solution containing SUVs and 200 µL of the buffer were mixed and added on a glass slide and incubated at 65^{o}C for 45 minutes-1 hour and left to cool to room temperature for another hour. The unfused vesicles were washed by draining and adding 100 µL of buffer repeatedly for 50-70 times using the buffer. Finally, the buffer amount was replenished and measurements were made.

Cell Culture

Cunningham's medium was prepared containing penicillin/streptomycin, gentamicin, hygromycin, neomycin and fetal bovine serum. The medium was filtered through 0.22µm filters by vacuum. The cells are maintained by passaging every alternate day by diluting the trypanosome suspension by 15 times and adding the selection drugs of phleomycin and blasticidin for the YFP-Procyclin CC2D RNAi *T. brucei*, blasticidin for the YFP-Procyclin *T. brucei* and phleomycin for CC2D RNAi *T. brucei* to maintain homogeneity of the type of *T. brucei*.

Agar Plate Preparation

0.4 g of low melting point agarose powder (BioRad, California, USA) was measured and added into a 125 mL flask. 5 mL distilled water was added. The flask was covered with Kimwipe and was put into a beaker with ~200 mL water. The entire set-up (flask+water bath) was heated in the microwave oven for 2 minutes or until water bath started to boil. It was left in the microwave for 1 minute and heated again for 15 seconds. The set-up was transferred to tissue culture hood and the water was left to cool to ~55^{o}C. 10 mL of fresh phenol-red free medium was added into the flask, mixed by pipetting it up and down several times (many bubbles should not be introduced). Another 15 mL of fresh medium was added, and the pipetting was repeated. Finally, 25 mL medium was added, mixed by pipetting, swirling and left in the water bath (~40 ^{o}C) for 2 minutes. The agarose should not solidify at temperature above 37^{o}C. Meanwhile, fifteen 35 mm petri-dishes were prepared in the hood. A 5 mL pipette was used and 3 mL of agarose was added into each petri-dish, covered and set aside in single layer at the back of the hood. Once the agarose was set (in 30-60 min) and dried for 30 min and each plate was wrapped with parafilm. The plates were stored at 4 ^{o}C for up to a month.

DiI-C_{18} Staining of Trypanosomes

The required population of trypanosomes (~1 million/mL) was centrifuged at 4600rpm and pelleted the CC2D RNAi *Trypanosoma brucei*. Then they were washed once with TDB (trypanosome dilution buffer: 20 mM Na_2HPO_4, 2 mM NaH_2PO_4, pH 7.7, 20 mM glucose, 5 mM KCl, 80 mM NaCl, 1 mM $MgSO_4$) and then pelleted again. 100 nM of DiI-C_{18} dye was obtained by serial dilution in TDB and was mixed thoroughly with the pellet after centrifugation. The trypanosomes were incubated at 28 ^{o}C for 20-25 minutes and washed once with Cunningham medium without phenol red (clear medium) and concentrated to the required concentration (~5million/mL).

MβCD treatment

YFP-Procyclin /DiI-stained wild-type *Trypanosoma brucei* (~1 million/mL) were washed in clear medium once and centrifuged at 4600 rpm to a pellet form before adding 2.5 mM of methyl-β-cyclodextrin to concentrate the trypanosomes to required concentration (~5 million/mL) before doing sample preparation for zFCS. The trypanosomes were immediately measured within 1 hour before doing another batch for the repeat experiments.

CC2D-RNAi induction for CC2D mutants

CC2D-RNAi/YFP-Procyclin CC2D-RNAi culture flasks were added with 10mg/mL tetracyclin with $(1/1000)^{th}$ the volume of the culture flask and maintained regularly with the same cell culture procedure as mentioned above for a maximum of 72 hours.

Sample Preparation for zFCS

Agarose plates and a tube of conditioned medium were brought to $28^{o}C$ in a humidified, CO_2 incubator. The required population of trypanosomes (~1 million/mL) was centrifuged at 4600rpm and pelleted. The supernatant was removed and the cells were washed with clear medium. Suitable amount of concentrated *Trypanosoma brucei* (~5 million/mL) of the cell suspension was added to the surface of an agarose plate and spread by rotating/swirling the plate until the liquid covers the entire surface. The extra liquid was removed. The cover was removed and the sample air dried in the hood until desired level of movement of trypanosomes is observed. Once the cells are immobilized, a piece was quickly cut from the agarose plate and inverted onto an imaging chamber with a cover glass bottom (Mattek; No.1; coverslip thickness 1.3-1.6 mm; Type C). The chamber was sealed or water was added to the side to slow down evaporation. Measurements were done within 1-1.5 hours of sample preparation to

ensure FCS readings were not taken from dead trypanosomes. DAPI staining can indicates whether the trypanosome is alive.

Calibration curves for FCS

The autocorrelation curve for Rhodamine 6G and Atto 565 are shown in Fig. 6. The diffusion coefficients are 414 $\mu m^2 s^{-1}$ and 426 $\mu m^2 s^{-1}$ respectively (Müller et al., 2008). With given coefficients and the diffusion time found from the autocorrelation functions fitted, the dimensions of the confocal volume can be found. The dimension of interest was the spot radius (r_0), from which the observation area was found for the 515 nm and 543 nm laser spots. The diffusion time of Rhodamine 6G was 21.7 µs which gives the spot radius of the 515 nm laser to be ~190 nm solving from equation 5. The diffusion time of Atto565 was found to be 24.5 µs which gives the spot radius of the 543 nm laser to be ~204 nm from equation 5.

A

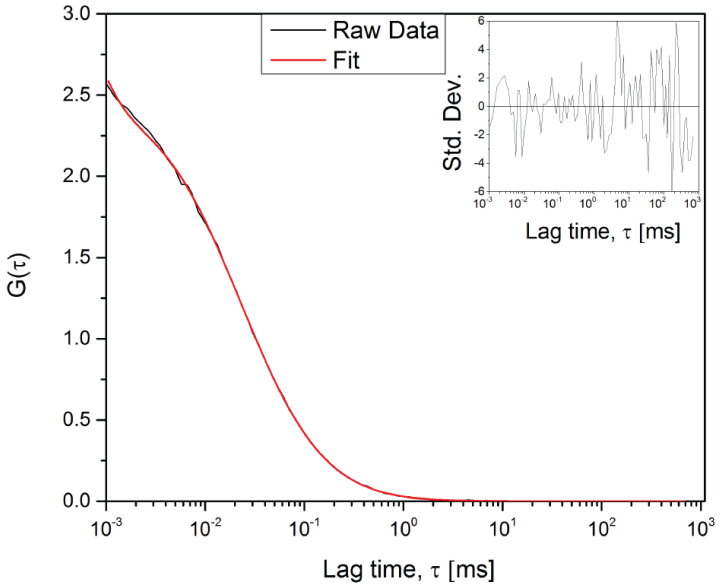

B

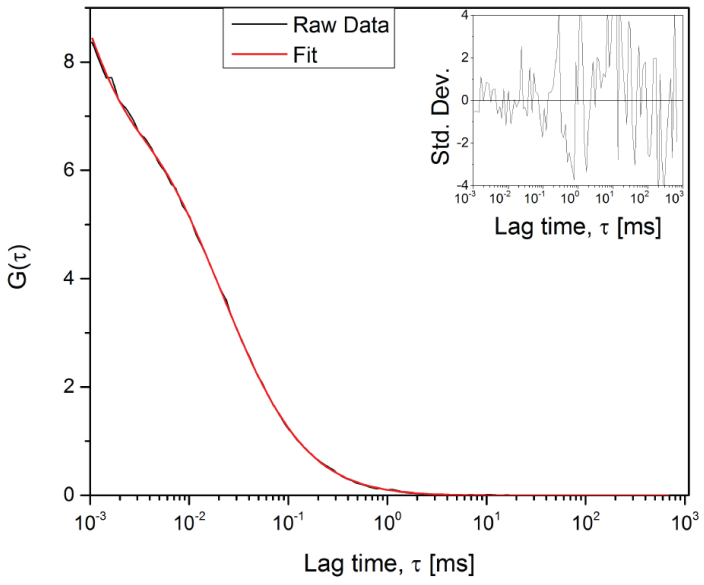

Fig. 6. Autocorrelation functions of Rhodamine 6G (A) and Atto565 (B) for calibration of focal volume. The residuals are given in the inset.

Results

Calibration of zero-spot width for zFCS using freely diffusing POPC bilayer

A linear plot of τ_D vs Δz^2, upon fitting and extrapolating to $\tau_D = 0$, we can find out the reference point, i.e. Δz^2 value on the negative x-axis. This value corresponds to the zero-spot width corresponding to our optical system. Such a calibration can be done using a well-defined system such as supported lipid bilayers. Rhodamine-PE in POPC bilayers is known to be freely diffusing at room temperature (Bag et al., 2012). Fig. 7 depicts the plot of τ_D with Δz. The diffusion coefficient obtained at $\Delta z = 0$, i.e. when the bilayer surface is at focus is ~3.5 $\mu m^2 s^{-1}$ which is faster than previously reported values (Bag et al., 2012). Such variation has also been observed using different techniques for the same kind of bilayer. Imperfections in bilayer preparation have a major contribution in the variability of diffusion coefficients obtained (Guo et al., 2008). The plot of τ_D with Δz^2 in Fig. 7 gives us the FCS diffusion law, the fit gives us the zero-spot width at Δz^2 = -0.092 μm^2. All comparisons in the subsequent diffusion law plots including τ_0 values will be interpreted with this Δz^2 value as the zero spot-width. The Δz^2 have been recalculated to r^2 using equation 10 to depict the diffusion laws.

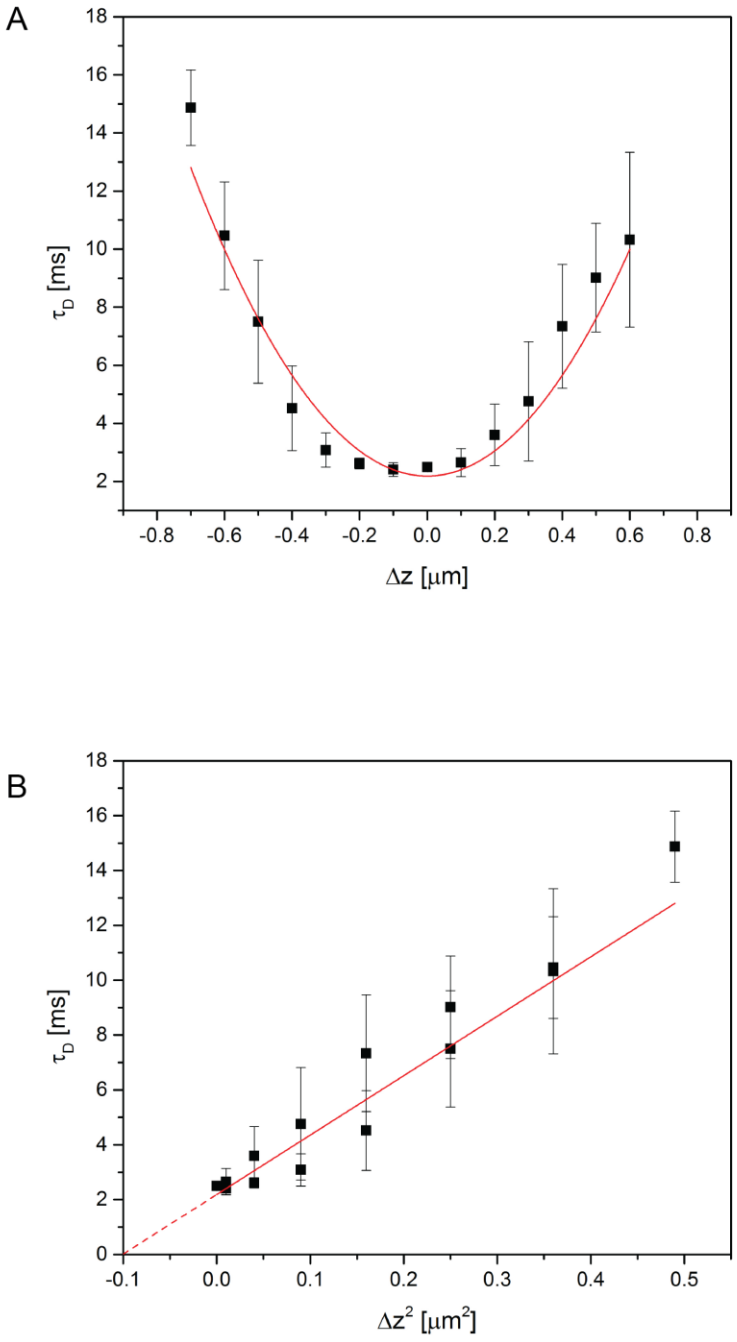

Fig. 7. zFCS Calibration using POPC bilayers. A. The parabolic dependence of the diffusion time, τ_D with change in z-position, Δz is given. We expect a symmetric parabola from Equation 7. **B.** The diffusion law plot of τ_D vs Δz^2 is given. Extrapolating the Δz^2 value we get -0.092 μm^2 for $\tau_D = 0$. $N_{exp} = 7$

YFP-Procyclin exhibits domain confinement in *T. brucei* plasma membrane

YFP-tagged procyclin was used to probe the membrane dynamics. DiI-C_{18}- stained trypanosomes have been used as control experiments as it is known to bind to the freely diffusing regime of the plasma membrane (Sot, J., Bagatolli, L.A., Alonso, A., 2006). For YFP-Procyclin, diffusion coefficient obtained at $\Delta z = 0$ is 1.0 $\mu m^2 s^{-1}$ with a standard deviation of 0.5 $\mu m^2 s^{-1}$. The diffusion law plot of τ_D with r^2 at zero spot-width gives an intercept of ~6.3 ms; this is the confinement time which is indicative of domain confinement (Wawrezinieck et al., 2005).

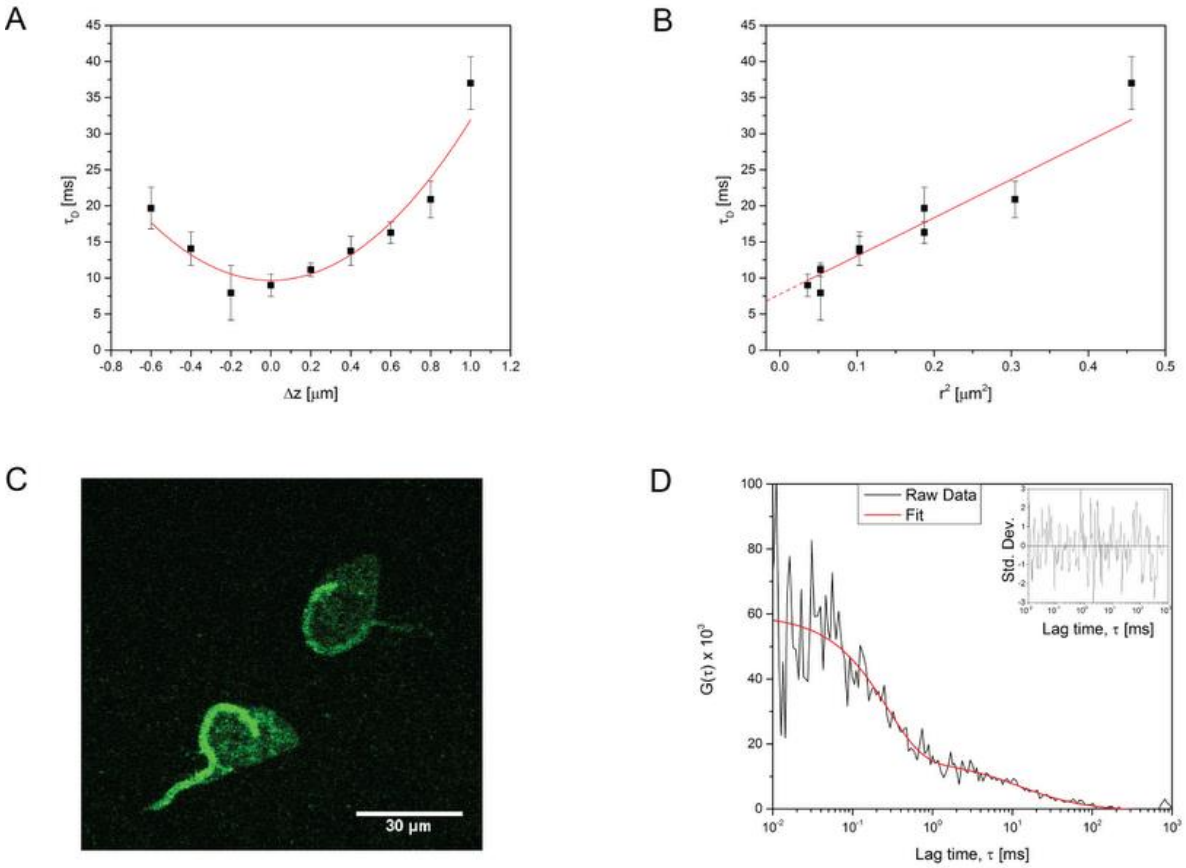

Fig. 8. zFCS and FCS Diffusion Law of YFP-Procyclin. A. The parabolic dependence of the diffusion time, τ_D with change in z-position, Δz is given. **B.** The diffusion law plot of τ_D vs r^2 is given. Extrapolating the diffusion law plot we get τ_0 = 6.8 ms. **C.** A fast scan image from the confocal microscope depicting the trypanosomes. **D.** A representative autocorrelation curve for YFP-Procyclin. The inset depicts the residuals of fit. N_{exp} = 4

Depletion of cholesterol using MβCD reduces domain confinement of procyclin

MβCD is known for depletion of cholesterol on the membrane in cells (Simons and Toomre, 2000; Zidovetzki and Levitan, 2007). Upon depletion of cholesterol using 2.5 mM MβCD, the confinement time decreased from ~6.3 ms to ~1.1 ms as shown in the diffusion law plot in Fig. 9. This is an indication that procyclin, from a regime of domain-confined diffusion has moved into a regime of free diffusion (Wawrezinieck et al., 2005). There is an increase in the diffusion coefficient from 1.0 $\mu m^2 s^{-1}$ to 2.4 $\mu m^2 s^{-1}$ with a standard deviation of 0.9 $\mu m^2 s^{-1}$ as shown in Fig. 9. Here it has been shown that procyclin indeed is confined to cholesterol-rich nanodomains and upon depletion of membrane cholesterol, the diffusion coefficient increases and confinement time decreases into the free diffusion regime.

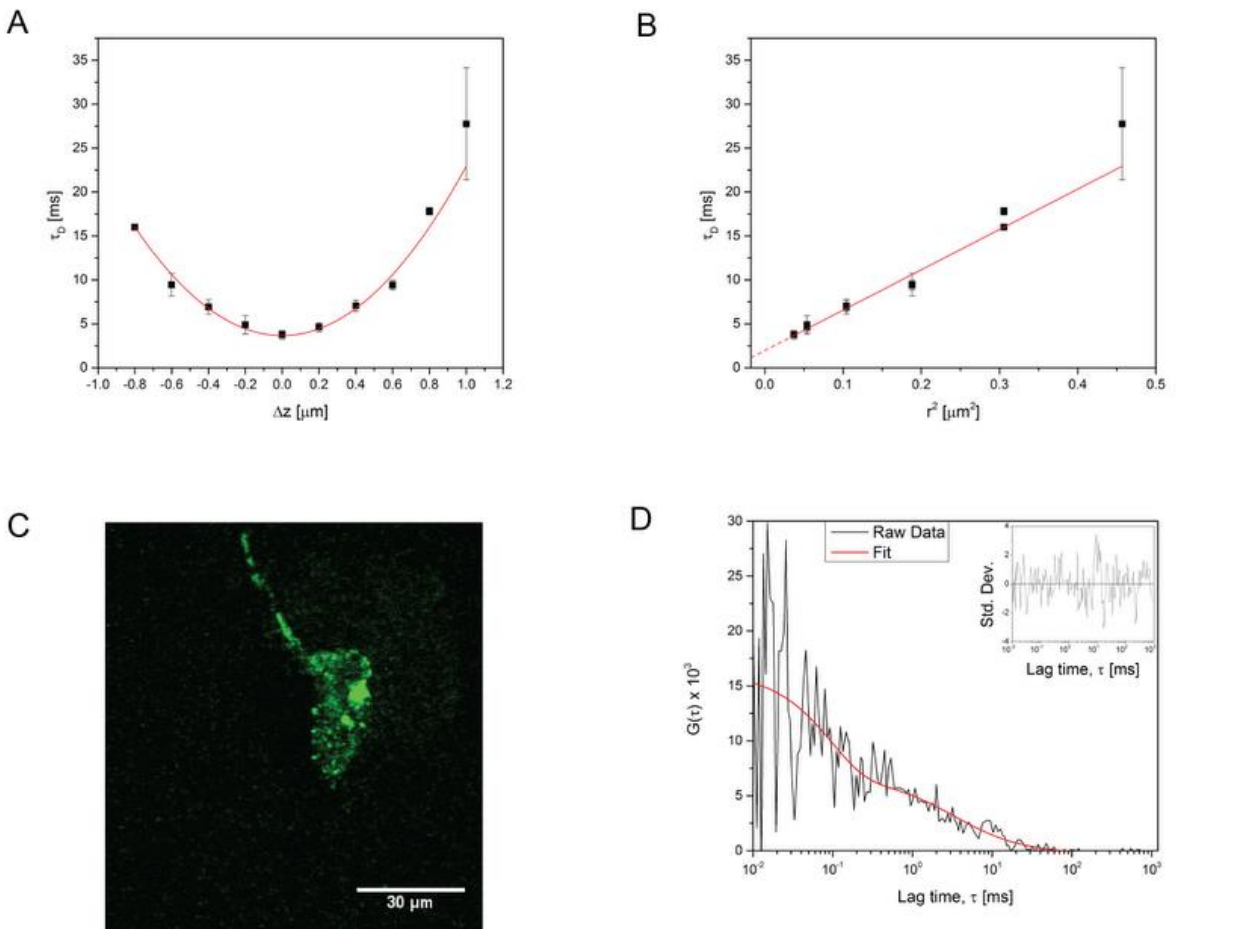

Fig. 9. zFCS and FCS Diffusion Law of YFP-Procyclin treated with MβCD. A. The parabolic dependence of the diffusion time, τ_D with change in z-position, Δz is given. **B.** The diffusion law plot of τ_D vs r^2 is given. Extrapolating the diffusion law plot we get τ_0 = 1.6 ms. **C.** A fast scan image from the confocal microscope depicting the trypanosomes after treatment with MβCD. **D.** A representative autocorrelation curve for YFP-Procyclin treated with MβCD. The inset depicts the residuals of fit. N_{exp} = 4

Knockdown of CC2D by RNA interference is similar to cholesterol depletion by MBCD

zFCS was performed upon knocking down the CC2D by RNA interference. Measurements were done 24 hours and 48 hours post knock down. Fig. 10. depicts the

plot of τ_D with Δz for 24 hours post knockdown. There is a decrease in the confinement time from ~6.3 ms to ~2.9 ms as shown in the diffusion law plot in Fig. 10 and and bar graph in Fig. 13. The diffusion coefficient increased from 1.0 $\mu m^2 s^{-1}$ to 2.6 $\mu m^2 s^{-1}$ with a standard deviation of 0.6 $\mu m^2 s^{-1}$ as shown in Fig.10. This shows a decrease in domain confinement of procyclin to a more freely diffusing regime. Similarly, 48 hours post knockdown the confinement time reduced to ~1.7 ms as shown in the diffusion law plot in Fig. 11 and bar graph in Fig. 13. The diffusion coefficient increased to 2.5 $\mu m^2 s^{-1}$.

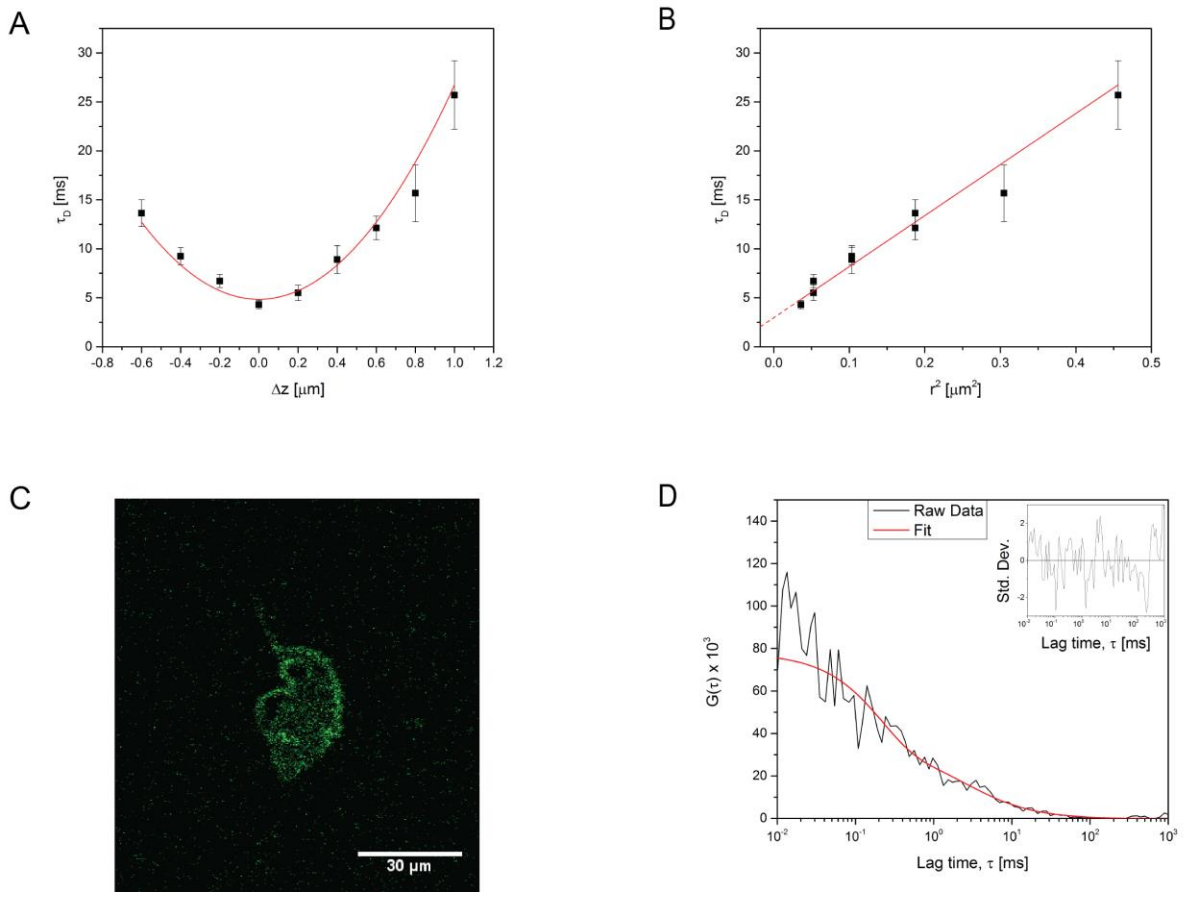

Fig. 10. zFCS and FCS Diffusion Law of YFP-Procyclin after 24 hours post CC2D knockdown using RNA interference. A. The parabolic dependence of the diffusion time, τ_D with change in z-position, Δz is given. **B.** The diffusion law plot of τ_D vs r^2 is given. Extrapolating the diffusion law plot we get τ_0 = 2.1 ms. **C.** A fast scan image from the confocal microscope depicting the trypanosomes after CC2D-RNAi induction for 24 hours. **D.** A representative autocorrelation curve for YFP-Procyclin after CC2D-RNAi induction for 24 hours. The inset depicts the residuals of fit. N_{exp} = 4

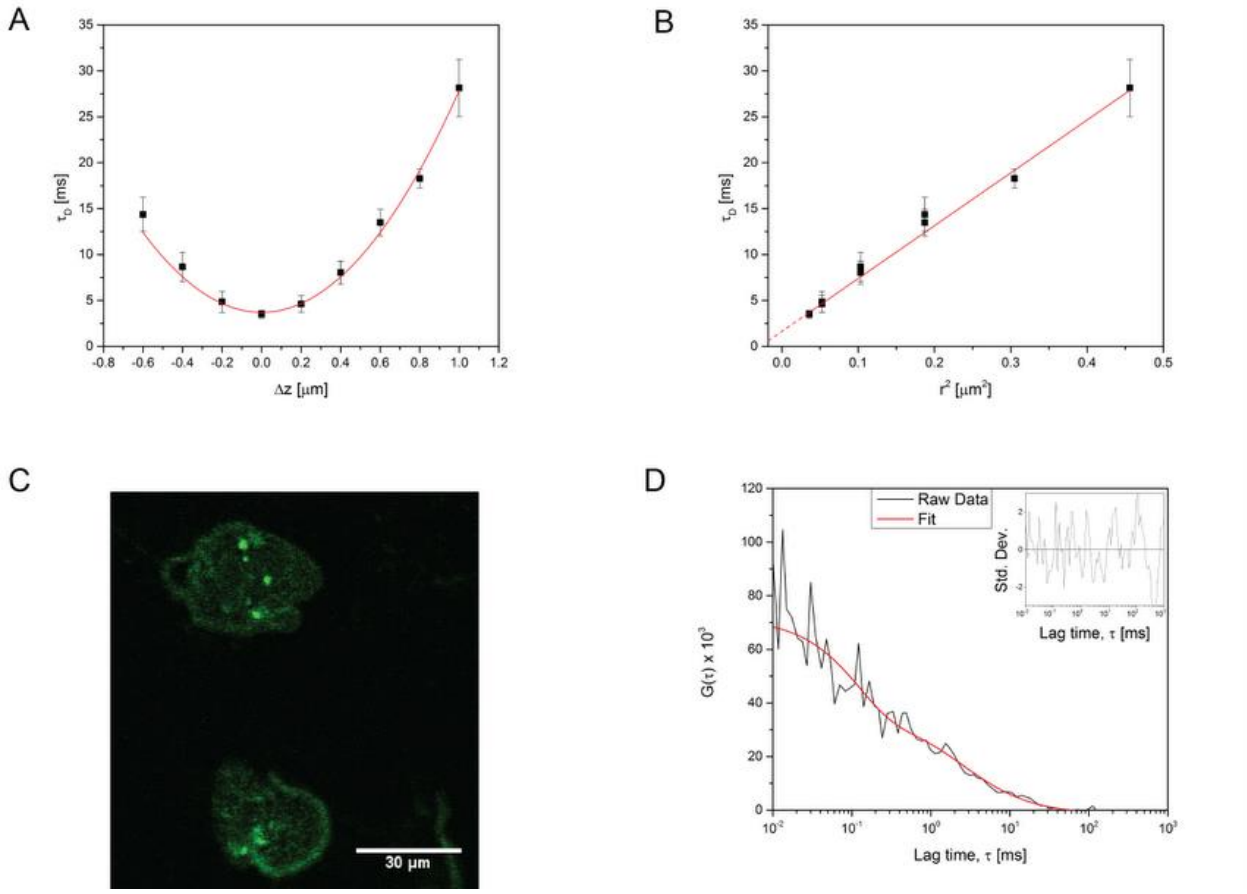

Fig. 11. zFCS and FCS Diffusion Law of YFP-Procyclin after 48 hours post CC2D knockdown using RNA interference. A. The parabolic dependence of the diffusion time, τ_D with change in z-position, Δz is given. **B.** The diffusion law plot of τ_D vs r^2 is given. Extrapolating the diffusion law plot we get τ_0 = 0.6 ms. **C.** A fast scan image from the confocal microscope depicting the trypanosomes after CC2D-RNAi induction for 48 hours. **D.** A representative autocorrelation curve for YFP-Procyclin after CC2D-RNAi induction for 48 hours. The inset depicts the residuals of fit. N_{exp} = 6

Discussion

Procyclin is a glycophosphoinositol (GPI) - anchored protein which preferentially partitions into the cholesterol-rich nanodomains of the cell membrane (Fielding and Fielding, 1997). It provides protection from the insect-host immune system and is the surface coat of the procyclic-form of the *Trypanosoma brucei*. The synthesis, transport and recycling of the GPI-anchored proteins is essential for effective protection by the surface coat and for these proteins, sterol and sphingolipids have a major effect on the dynamics (Muniz and Riezman, 2000; Muniz and Riezman 2016). The diffusion coefficient obtained for *Trypanosoma brucei* is faster compared to GFP-GPI measurements in HeLa cells which is ~0.17 $\mu m^2 s^{-1}$ and ~0.35 $\mu m^2 s^{-1}$ in SH-SY5Y cells at 398 K (Bag et al., 2013; Ng et al., 2016). SH-SY5Y cells show an increase to ~0.6 $\mu m^2 s^{-1}$ upon treatment with MβCD which is about a 100% percent increase in diffusion (Ng et al., 2016). Here we observed an increase of diffusion coefficient by about 140% upon treatment. Confinement in the case of procyclin was expected as GPI-anchored proteins are known to be associated to cholesterol-rich nanodomains (Fielding and Fielding, 1997). A decrease in confinement time and an increase in diffusion coefficient show that MβCD indeed is causing changes in the membrane distribution of procyclin.

The decrease of confinement time and increase in diffusion coefficient after CC2D knockdown is similar to that observed in the depletion of cholesterol by MβCD. There could be a correlation between cholesterol uptake on the plasma membrane and the knockdown of CC2D. Also, intensity traces while doing the FCS measurements showed higher intensity spikes more frequently (data not shown) upon MβCD treatment too. The images however showed no noticeable differences.

Depletion of cholesterol by different methods has shown to cause reduction in the expression of GPI-anchored proteins, dispersion of the proteins across the cell membrane, improvement of solubility in non-ionic detergents and protein signaling impairment (Ilangumaran and Hoessli, 1998). In Jurka T cells, it has been observed that calcium response by GPI-anchored proteins CD59 and CD48 signaling have been affected by cholesterol production impairment using different inhibitors (Stulnig et al., 1997). They reported that calcium release was inhibited in the intracellular stores by the

inhibition of cholesterol. Though they did not observe any decrease in cell-surface expression. Also, given that GPI-anchored proteins do not contain a transmembrane domain, it is likely that for signaling, they would be clustered together. Cholesterol depletion has been shown to reduce Fyn-signaling upon addition of its effector, TSP-1 in human microvascular endothelial cells related to the endothelial cell surface receptor, CD36 (Githaka et al., 2016). Hence, there is a possibility of signaling being affected by reduction of cholesterol in *Trypanosoma brucei*.

However, membrane size control and cholesterol depletion correlation is yet to be understood, at least in the case of *Trypanosoma brucei*.

The procyclic-form of *T.* brucei acquires sterols from both endogeneous (sterol biosynthesis) and exogeneous (lipoprotein endocytosis) sources. These two processes work hand-in-hand to maintain a sort of sterol homeostasis by regulating each other (Coppens and Courtoy, 2000). One hypothesis is that there is a problem in the uptake of cholesterol by endocytosis. The endocytotic apparatus is concentrated between the flagellar pocket and the nucleus. Unlike the bloodstream form where the main source of sterols is from the endocytosis of low density lipoproteins (LDL), procyclic form can also produce these *de novo* from an intermediate. Cholesterol is generally endocytosed but when there is lack of LDL proteins, ergosterol is predominantly produced in the procyclic forms. Once the procyclic forms have excess cholesterol accumulation from the uptake of LDL, the cholesterol is converted to cholesterol-ester, which is then stored. The amount of sterols esterified is dependent on the sterol intake from the different pathways. The cholesterol esterification is mainly dependent on the exogeneous uptake rather than endogeneous synthesis (Coppens and Courtoy, 2000). One hypothesis is that there is a problem in the uptake of cholesterol by endocytosis from the lipoprotein-rich serum added in the medium essential for growth of trypanosomes upon knockdown of CC2D. The other hypothesis is that CC2D knockdown has implications in the endogeneous trafficking system of the trypanosomes where the sterols are not able to effectively get incorporated onto the membrane. Uptake and pulse-chase experiments of cholesterol from the surrounding environment would give an insight on the first

hypothesis presented here and fluorescence microscopy and quantitative analysis of different procyclin in the cytosol upon knockdown of CC2D can help give a better understanding of trafficking of these proteins correlating to the amount of cholesterol in the membrane. In summary, Figs. 12 and 13 and Tables 1 and 2 give a brief outline of the observations.

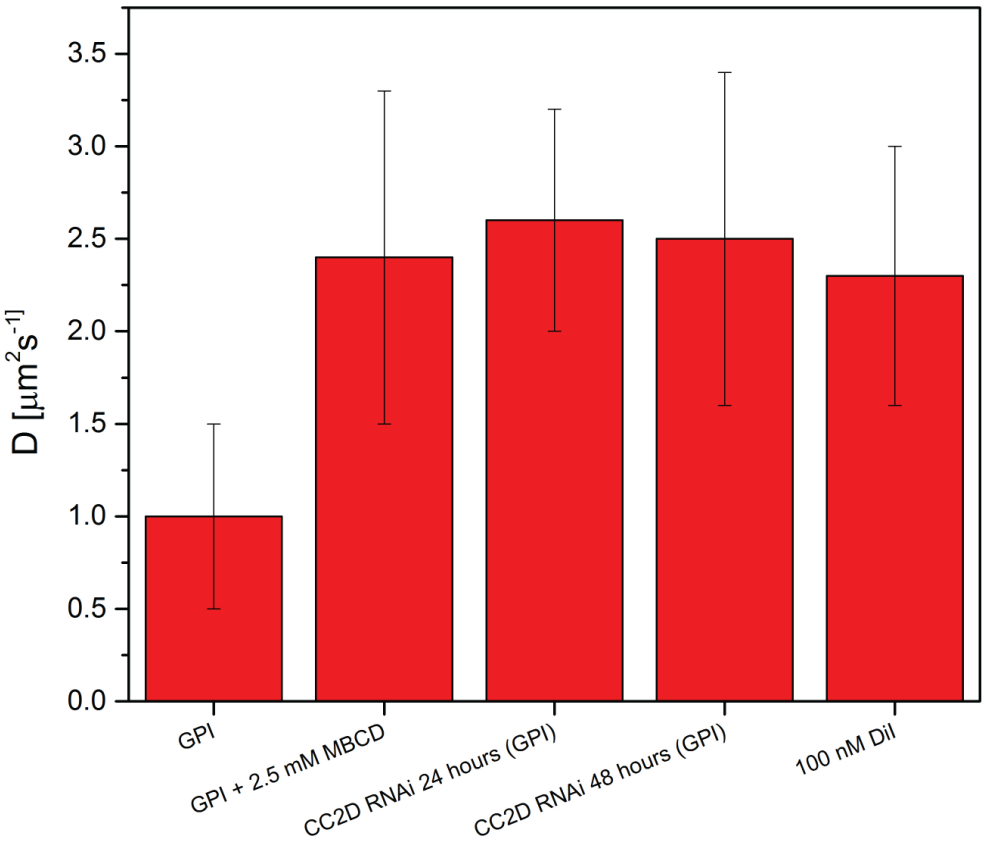

Fig.12. Diffusion coefficient measurements of different membrane markers on the plasma membrane of *T. brucei*. Given here are the different experiments done and their respective diffusion coefficients. D is the diffusion coefficient in $\mu m^2 s^{-1}$, the error bars are the standard deviations of the measurements. N_{exp} are given in Table. 1.

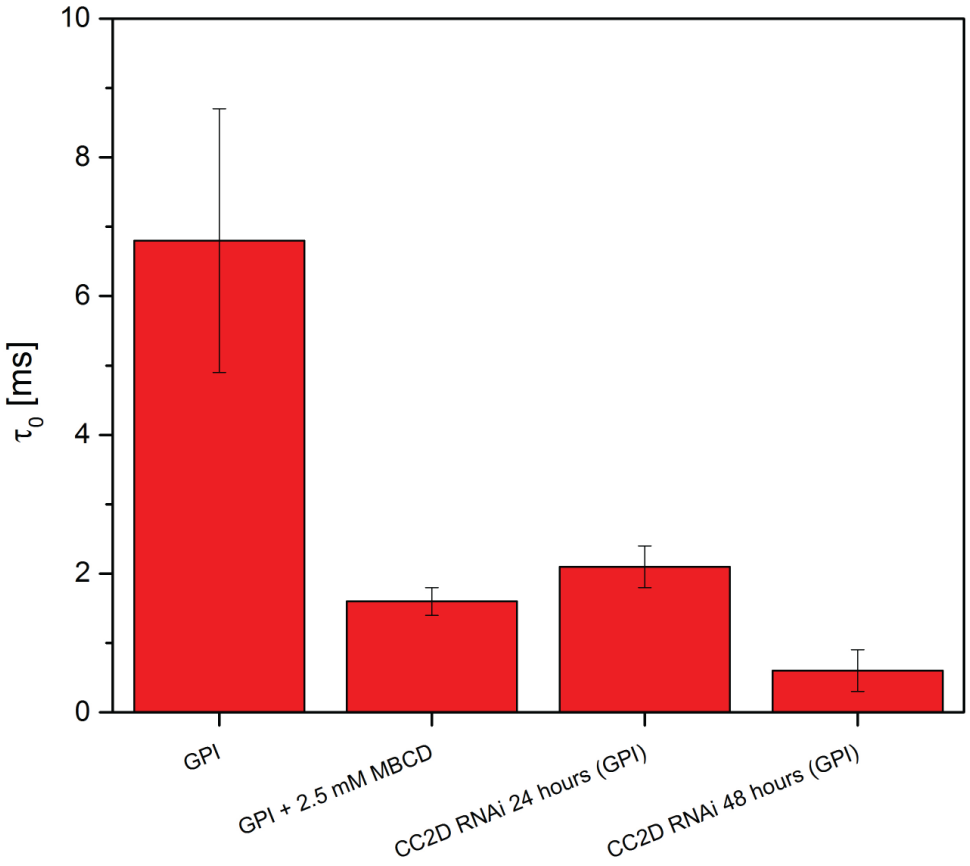

Fig. 13. τ_0 measurements obtained from FCS Diffusion Laws for different membrane markers on plasma membrane of *T. brucei*. Given here are the different experiments done and their respective confinement times. τ_0 is the confinement time in ms, the error bars represent the standard deviations of the measurements. N_{exp} are given in Table. 2.

Tables

	YFP-Procyclin	YFP-Procyclin + 2.5 mM MβCD	YFP-Procyclin CC2D RNAi 24 hours	YFP-Procyclin CC2D RNAi 48 hours	100 nM DiI
D ($\mu m^2 s^{-1}$)	**1**	**2.4**	**2.6**	**2.5**	**2.3**
Std dev ($\mu m^2 s^{-1}$)	**0.5**	**0.9**	**0.6**	**0.9**	**0.7**
N_{exp}	**38**	**26**	**29**	**26**	**22**

Table. 1. Diffusion coefficient measurements of different membrane markers on the plasma membrane of *T. brucei*. Given here are the different experiments done and their respective diffusion coefficients. D is the diffusion coefficient in $\mu m^2 s^{-1}$, Std. dev. is the standard deviations of the measurements done in $\mu m^2 s^{-1}$, N_{exp} is the number of experiments performed.

	YFP-Procyclin	YFP-Procyclin + 2.5 mM MβCD	YFP-Procyclin CC2D RNAi 24 hours	YFP-Procyclin CC2D RNAi 48 hours
τ_0 (ms)	**6.8**	**1.6**	**2.1**	**0.6**
Std dev (ms)	**1.9**	**0.2**	**0.3**	**0.3**
N_{exp}	**4**	**4**	**4**	**6**

Table. 2. τ_0 measurements obtained from FCS Diffusion Laws for different membrane markers on plasma membrane of *T. brucei*. Given here are the different experiments done and their respective confinement times. τ_0 is the confinement time in ms, Std. dev. is the standard deviations of the measurements done in ms, N_{exp} is the number of experiments performed.

Conclusion

Hence, we can conclude that membrane dynamics of Procyclin, a GPI-anchored protein after knockdown of CC2D by RNA interference resembles cholesterol depletion by MβCD on plasma membrane of *Trypanosoma brucei* by z-scan FCS and FCS Diffusion Laws. Such measurements have been done for the first time on this organism. These observations support the initial observations made with the filipin staining experiments described in the introduction.

References

Aragón, S. R., and Pecora, R. (1975). Fluorescence correlation spectroscopy and Brownian rotational diffusion. Biopolymers 14, 119–138.

Bag, N., Sankaran, J., Paul, A., Kraut, R., Wohland, T. (2012). Calibration and Limits of Camera-Based Fluorescence Correlation Spectroscopy: A Supported Lipid Bilayer Study. ChemPhysChem 13, 2784-2794.

Brian, A. A., McConnell, H. M. (1984). Allogeneic stimulation of cytotoxic T cells by supported planar membranes. PNAS 81, 6159-6163.

Cho, W., Stahelin, R.V. (2006). Membrane binding and subcellular targeting of C2 domains. Biochim Biophys Acta 1761(8), 838-849.

Coppens, I., Courtoy, P.J. (2000). The adaptive mechanisms of *Trypanosoma brucei* for sterol homeostasis in its different life-cycle environments. Annual Review of Microbiology vol 54, 129-145.

Elson, E. L., and Magde, D. (1974). Fluorescence correlation spectroscopy. I. Conceptual basis and theory. Biopolymers 13, 1–27.

Fielding, C.J., Fielding, P.E. (1997). Intracellular cholesterol transport. Journal of Lipid Research Volume 38, 1503-1521.

Garcia-Salcedo, J.A., Perez-Morga, D., Gijon, P., Dilbeck, V., Pays, E., Nolan, D.P. (2004). A differential role for actin during the life cycle of *Trypanosoma brucei*. EMBO J. 23(4), 780-789.

Githaka, J.M., Vega, A.R., Baird, M.A., Davidson, M.W., Jaqaman, K., Touret, N. (2016). Ligand-induced growth and compaction of CD36 nanoclusters enriched in Fyn induces Fyn signaling. Journal of Cell Science (129), 4175-4179.

Guo, L., Har, J.Y., Sankaran, J., Hong, Y., Kannan, B., Wohland, T. (2008). Molecular Diffusion Measurement in Lipid Bilayers over Wide Concentration Ranges: A Comparative Study. ChemPhysChem 9, 721-728.

Haustein, E., and Schwille, P. (2007). Fluorescence correlation spectroscopy: novel variations of an established technique. Annu. Rev. Biophys. Biomol. Struct. 36, 151–169.

Humpolícková, J., Gielen, E., Benda, A., Fagulova, V., Vercammen, J., vandeVen, M., Hof, M., Ameloot, M., Engelborghs, Y. (2006). Probing Diffusion Laws within Cellular Membranes by Z-Scan Fluorescence Correlation Spectroscopy. Biophysical Journal: Biophysical Letters , L23-L25.

Lacomble, S., Vaughan, S., Deghelt, M., Moreira-Leite, F.F., Gull, K. (2012). A *Trypanosoma brucei* protein required for maintenance of the flagellum attachment zone and flagellar pocket ER domains. Protist 163(4), 602-615.

Müller, C.B., Loman, A., Pacheco, V., Koberling, F., Willbold, D., Richtering, W., Enderlein, J. (2008). Precise measurement of diffusion by multi-color dual-focus fluorescence correlation spectroscopy. EPL 83(4).

Muniz, M., Riezman, H. (2000). Intracellular transport of GPI-anchored proteins. EMBO J. 19(1), 10-15.

Muniz, M., Riezman, H. (2016). Trafficking of glycosylphosphatidylinositol anchored proteins from the endoplasmic reticulum to the cell surface. J Lipid Res. 57(3), 352-360.

Ng, X.W., Bag, N., Wohland, T. (2015). Characterization of Lipid and Cell Membrane Organization by the Fluorescence Correlation Spectroscopy Diffusion Law. Chimia (Aarau). 69(3), 112-119.

Pike, L.J. (2006). Rafts defined: a report on the Keystone Symposium on Lipid Rafts and Cell Function. J. Lipid Res. 47, 1597.

Simons, K., Toomre, D. (2000). Lipid Rafts and Signal Transduction. Nature Rev. Mol. Cell Biol. 1(1), 31-39.

Sot, J., Bagatolli, L. A., Alonso, A. (2006). Detergent-resistant, ceramide-enriched domains in sphingomyelin/ceramide bilayers. Biophys. J. 90, 903–914.

Stulnig, T.M., Berger, M., Sigmund, T., Stockinger, H., Horejsi, V., Waldhausl, W. (1997). Signal Transduction via Glycosyl Phosphatidylinositol-anchored Proteins in T cells is inhibited by lower cellular Cholesterol. Journal of Biological Chemistry Vol. 272(31), 19242-19247.

Sunter, J.D., Varga, V., Dean, S., Gull, K. (2015). A dynamic coordination of flagellum and cytoplasmic cytoskeleton assembly specifies cell morphogenesis in trypanosomes. Journal of Cell Science 128(8), 1580-1594.

Tyler, K.M., Fridberg, A., Toriello, K.M., Olson, C.L., Cieslak, J.A., Hazlett, T.L., et al. (2009). Flagellar membrane localization via association with lipid rafts. Journal of Cell Science 122(6), 859-866.

Wawrezinieck, L., Rigneault, H., Marguet, D., Lenne, P-F. (2005). Fluorescence Correlation Spectroscopy Diffusion Laws to Probe the Submicron Cell Membrane Organization. Biophysical Journal Volume 89, 4029-4042.

Wenger, J., Conchonaud, F., P. F. Lenne, P. F. (2007). Diffusion analysis within single nanometric apertures reveals the ultrafine cell membrane organization. Biophys. J. 92. 913–919.

Yechiel, E., Edidin, M. (1987). Micrometer-scale domains in Fibroblast Plasma Membranes. Journal of Cell Biology Volume 105, 755-760.

Zhou, Q., Liu, B., Sun, Y., He, C.Y. (2011). A coiled-coil- and C2-domain-containing protein is required for FAZ assembly and cell morphology in *Trypanosoma brucei*. Journal of Cell Science 124(22), 3848-3858.

Zhao, M., Jin, L., Chen, B., Ding, Y., Ma, H., Chen, D. (2003). Afterpulsing and its correlation in fluorescence correlation spectroscopy experiments. Applied Optics Volume 42(19), 4031-4036.

Zidovetzki, R., and Levitan, I. (2007). Use of cyclodextrins to manipulate plasma membrane cholesterol content: evidence, misconceptions and control strategies. Biochim. Biophys. Acta. 1768, 1311–1324.